Correction

PSYCHOLOGICAL AND COGNITIVE SCIENCES

Correction for "Exposure therapy triggers lasting reorganization of neural fear processing," by Katherina K. Hauner, Susan Mineka, Joel L. Voss, and Ken A. Paller, which appeared in issue 23, June 5, 2012, of *Proc Natl Acad Sci USA* (109:9203-9208; first published May 23, 2012; 10.1073/pnas.1205242109).

The authors note that the x/y/z coordinates listed for brain regions in Table 1 appeared incorrectly. The corrected table appears below. This error does not affect the conclusions of the article.

Table 1. Summary of fMRI activity clusters

						Baseline, phobogenic vs. neutral		Baseline vs. posttherapy		Posttherapy vs. follow-up	
Region (BA)	L/R/B	Volume (mm^3)	*x*	*y*	*z*	*t*	*P*	*t*	*P*	*t*	*P*
Fig 1. regions shown in blue											
Posterior cingulate (BA 31)	B	8,343	4	−40	49	1.77	0.10	−2.82	0.02	2.03	0.07
Anterior cingulate/ vmPFC (BA 24, 32)	B	7,965	−3	20	27	3.19	0.01	−3.11	0.01	NS	
Anterior insula (BA 13)	L	2,187	−53	8	−1	2.09	0.06	−2.70	0.02	NS	
Anterior insula (BA 13)	R	1,782	37	6	6	3.91	0.00	−2.46	0.03	NS	
Posterior insula (BA 13, 19)	R	8,478	47	−45	13	2.33	0.04	−2.81	0.02	NS	
Middle temporal gyrus (BA 39)	L	1,134	−41	−51	7	3.77	0.00	−2.71	0.02	NS	
Medial frontal gyrus (BA 6)	R	1,809	6	−15	67	2.68	0.02	−2.48	0.03	NS	
Amygdala (anatomically defined)	R	891	n/a	n/a	n/a	3.65	0.00	−4.59	0.00	NS	
Fig 1. region shown in red											
dlPFC (BA 6, 8)	R	918	36	15	61	−2.38	0.04	8.27	0.00	−2.63	0.02
Superior parietal lobule (BA 7)	R	1,458	25	−72	57	NS		3.12	0.01	NS	
Fig. 2 regions shown in gray											
Fusiform/lingual gyrus (BA 18, 19)	L	8,046	−34	−81	−9	4.91	0.00	NS		−5.10	0.00
Fusiform/lingual gyrus (BA 18, 19)	R	11,367	36	−78	−11	5.14	0.00	NS		−5.36	0.00

For each activity cluster, listed are Brodmann areas (BA), hemisphere [left (L), right (R), or bilateral (B)], the volume (mm^3), and stereotactic coordinates for the centrally activated voxel (*x, y, z* mm). Statistics are reported for all *P* values ≤ 0.10, and otherwise listed as nonsignificant (NS).

www.pnas.org/cgi/doi/10.1073/pnas.1210927109

Exposure therapy triggers lasting reorganization of neural fear processing

Katherina K. Hauner[a,b,1], Susan Mineka[b], Joel L. Voss[c,d], and Ken A. Paller[b,d]

[a]Department of Neurology, [c]Department of Medical Social Sciences, and [d]Interdepartmental Neuroscience Program, Feinberg School of Medicine, Northwestern University, Chicago, IL 60611; and [b]Department of Psychology, Northwestern University, Evanston, IL 60208

Edited by Mortimer Mishkin, National Institute of Mental Health, Bethesda, MD, and approved April 24, 2012 (received for review March 28, 2012)

A single session of exposure therapy can eliminate recalcitrant and disabling fear of phobogenic objects or situations. We studied neural mechanisms of this remarkable outcome by monitoring changes in brain activity as a result of successful 2-h treatment. Before treatment, phobogenic images excited activity in a network of regions, including amygdala, insula, and cingulate cortex, relative to neutral images. Successful therapy dampened responsiveness in this fear-sensitive network while concomitantly heightening prefrontal involvement. Six months later, dampened fear-network activity persisted but without prefrontal engagement. Additionally, individual differences in the magnitude of visual cortex activations recorded shortly after therapy predicted therapeutic outcomes 6 mo later, which involved persistently diminished visual responsiveness to phobogenic images. Successful therapy thus entailed stable reorganization of neural responses to initially feared stimuli. These effects were linked to fear-extinction mechanisms identified in animal models, thus opening new opportunities for the treatment and prevention of debilitating anxiety disorders.

emotion | functional MRI | specific phobia

The anxiety disorder known as "specific phobia" is characterized by intense, persistent, and excessive fear of an object or situation (1). This fear can be so disabling that sufferers restructure aspects of their lives to avoid it. However, some anxiety disorders, phobias in particular, can be eliminated in mere hours via one session of exposure therapy (2–4). Exposure therapy is an effective clinical intervention based on progressive confrontation with the pathologically feared stimuli (5). Approximately 95% of patients treated for phobia in one several-hour session maintain significant improvement in symptoms after 1 y (2, 3). Despite abundant evidence supporting the efficacy of exposure therapy, the neurophysiological mechanisms by which it reduces fear have yet to be discovered (6).

Exposure therapy is derived from principles of classical conditioning (5, 7). Fear can be conditioned by pairing a neutral stimulus with an aversive stimulus until the neutral stimulus alone elicits a fear response. Conditioned fear can then be extinguished by repeatedly presenting the neutral stimulus alone until the fear response is diminished. Both fear learning and fear extinction involve the amygdala (8), but only fear extinction is thought to also involve recruitment of the prefrontal cortex (PFC) for inhibition of fear-related amygdala processing (7, 9–11). Although conditioned fear in nonhuman animals arguably provides a suitable model for anxiety disorder (8), evidence is lacking to directly link such neurophysiological mechanisms with the presentation and treatment of phobic symptoms in human patients (6).

An important feature of fear extinction in both human and nonhuman animals is its time course, as fear extinction is not instantaneous. Rather, a process of consolidation is essential for stabilizing the fear-extinction memory (12, 13). Opposing views of how consolidation serves to sustain fear extinction have been suggested. Consolidation may entail the strengthening of "top-down" influences whereby cognitive control is exerted over fear responses via PFC-mediated inhibition of the amygdala (11, 14, 15). Alternatively, consolidation may depend on "bottom-up" influences, such as changes in sensory processing of feared stimuli. Whereas the amygdala can facilitate threat detection by enhancing sensitivity for sensory processing of feared stimuli (16, 17), a gradual reduction in fear may involve restructured connectivity between sensory-processing networks and the amygdala. Understanding these putative mechanisms in the context of exposure therapy requires analyzing both immediate and long-term neural consequences of this treatment.

Single-session exposure therapy presents a valuable opportunity whereby immediate changes in neural processing of feared stimuli can be identified and compared with long-term changes. To accomplish this comparison, we used functional MRI (fMRI) to observe neural processing of phobogenic images in adult volunteers who were successfully treated for spider phobia with single-session exposure therapy. Neural responses to phobogenic (versus neutral) images were assessed immediately before and after single-session exposure therapy, and again during a 6-mo follow-up visit. These procedures allowed us to provide a unique comparison of initial alterations caused by therapy with neural reorganization maintained over time.

Results

During all fMRI scanning sessions, neural activity elicited by phobogenic images (spiders) was computed relative to that elicited by neutral images (moths). This strategy allowed us to eliminate nonspecific effects common to both stimulus categories (e.g., visual stimulation, perceptual processing), so as to isolate activity related specifically to processing phobogenic images. Subjects performed a challenging visual detection task to ensure careful foveal processing of all images. The initial scanning session provided a baseline against which to assess neural changes due to treatment. At baseline, self-reported fear ratings collected during scanning (Fig. 1*A*) were significantly higher for phobogenic versus neutral stimuli [$t(11) = 15.55$, $P < 0.0001$]. As expected, brain activity for phobogenic versus neutral images was greater in limbic, paralimbic, and related regions, including right amygdala, bilateral insula, and cingulate cortex (Fig. 1 *B* and *C*, shown in blue, Table 1, and Fig. S1).

Despite lifetime histories of spider phobia, all subjects were successfully treated within 3 h or less. Therapy involved a progressive series of tasks to approach the live tarantula, with each step first demonstrated by the therapist (18). Reduced fear after treatment was evident in decreased ratings on two standard questionnaires (19, 20), subjects' ability to approach and touch the tarantula, and decreased fear ratings during scanning (all $P < 0.001$) (Fig. 1*A*).

Author contributions: K.K.H., S.M., J.L.V., and K.A.P. designed research; K.K.H. performed research; K.K.H. analyzed data; and K.K.H., S.M., J.L.V., and K.A.P. wrote the paper.

The authors declare no conflict of interest.

This article is a PNAS Direct Submission.

[1]To whom correspondence should be addressed. E-mail: hauner@u.northwestern.edu.

This article contains supporting information online at www.pnas.org/lookup/suppl/doi:10.1073/pnas.1205242109/-/DCSupplemental.

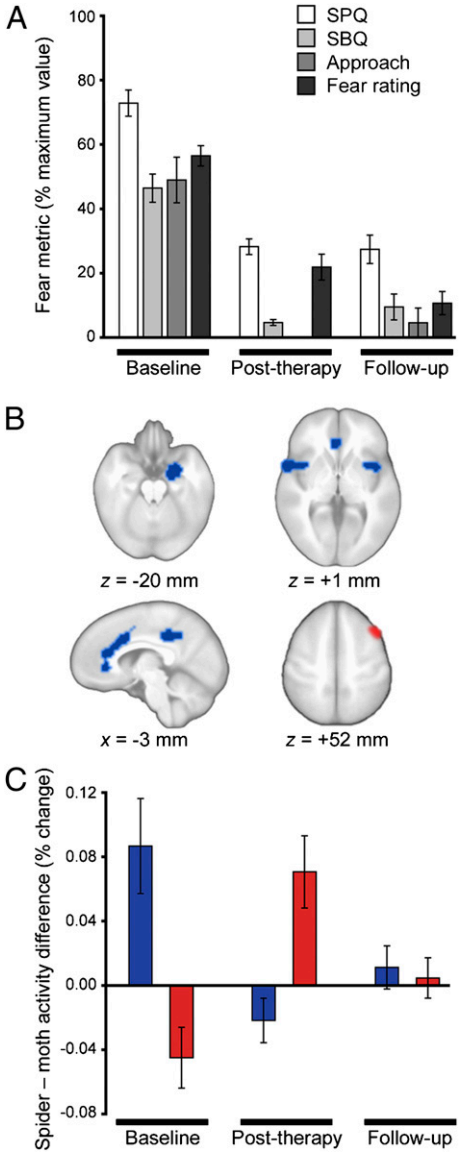

Fig. 1. Exposure therapy reduced fear and changed neural processing of phobogenic images. (*A*) Mean values for the four behavioral fear indices showed high fear of spiders at baseline, a reduction after exposure therapy, and an enduring reduction at 6-mo follow-up (despite no continued therapy). Values are shown as a percentage of the maximum score possible for each fear index (see *Materials and Methods*). (*B*) Brain activations are shown superimposed on a standard brain template. Regions shown in blue (darker) indicate significantly greater activity at baseline (for phobogenic versus neutral images) that decreased significantly as a result of therapy, as described in Table 1. The averaged location of right amygdala across subjects is indicated in standard stereotactic space (at $z = -20$ mm). The dlPFC region showing significantly decreased activity at baseline (for phobogenic versus neutral images) and significantly increased activity as a result of therapy (Table 1) is shown in red (lighter). (*C*) Mean activity is shown separately for the red region and for blue regions during the baseline, posttherapy, and follow-up scans. Estimates shown in blue (darker) correspond to the mean of all regions shown in blue in *B*, weighted by region volume. Activity for each region shown in blue appears individually in Fig. S1. Error bars indicate SEM. Activity in each individual region is summarized in Table 1.

Reduced fear after therapy was accompanied by several distinct changes in neural activity. Right dorsolateral PFC (dlPFC) showed significantly increased activity for phobogenic versus neutral images during the posttherapy scan [$t(11) = 3.15$, $P = 0.009$] (Fig. 1 *B* and *C*, shown in red), despite having previously shown the opposite pattern at baseline (significantly decreased activity for phobogenic versus neutral images) (Fig. 1*C* and Table 1). This pattern is consistent with the dlPFC's hypothesized role in emotional self-regulation (21) and cognitive reappraisal (22, 23). Concomitant with dlPFC increases, initially fear-responsive regions, including amygdala, insula, cingulate cortex, and ventromedial PFC (vmPFC), showed activity decreases, such that they no longer exhibited greater activity for phobogenic versus neutral images (Fig. 1 *B* and *C*, shown in blue, Table 1, and Fig. S1). In addition, right superior parietal lobule, which did not show differential responses to phobogenic versus neutral images at baseline, exhibited greater activity for phobogenic images following treatment [$t(11) = 5.52$, $P = 0.0002$] (Table 1), potentially signaling heightened visuo-spatial attention (24).

These posttherapy changes in neural processing of phobogenic images, however, could potentially be attributed merely to repeated scanning procedures or to the passage of time rather than to the effects of therapy. To assess this possibility, we scanned half of the subjects on two occasions before therapy–at baseline and following a 2-h waiting period. In this wait-group subsample, none of the four behavioral measures of fear significantly differed between the baseline and postwait assessments; however, all four measures did significantly decrease between the postwait and posttherapy assessments (Fig. S2*A*). In addition, comparisons of neural activity during the baseline, postwait, and posttherapy scans demonstrated that changes observed after therapy were not produced merely by repeating the fMRI scanning procedures following the waiting period, but rather selectively reflected the exposure-therapy manipulation (Fig. S2*B*). Within the wait group itself, changes in neural activity from postwait to posttherapy scans [$F(1,64) = 9.95$, $P = 0.002$, regions shown in blue (Fig. S2*B*); $F(1,8) = 4.61$, $P = 0.06$, dlPFC shown in red (Fig. S2*B*)] indicated that the lack of change between the baseline and postwait scans [$F(1,64) = 0.01$, $P = 0.93$; $F(1,8) = 0.54$, $P = 0.48$; blue regions and dlPFC, respectively (Fig. S2*B*)] was not a result of reduced sample size relative to the full sample. Rather, changes in behavior and brain activity were caused selectively by therapy.

Despite a 6-mo absence of further therapeutic intervention, subjects maintained therapy gains and showed fear assessments at follow-up comparable to those observed immediately after therapy (Fig. 1*A*). No subject met criteria for spider phobia at follow-up. Correspondingly, many of the neural changes observed immediately after therapy were also maintained. Amygdala/limbic areas that had been more active at baseline for phobogenic images and that showed immediate posttherapy decreases (shown in blue in Fig. 1*B*) continued to exhibit this decreased activity to phobogenic images at follow-up, showing no significant differences between posttherapy and follow-up scans (Fig. 1*C*, Table 1, and Fig. S1).

In contrast, there was a significant reduction in dlPFC activity from posttherapy to follow-up [$t(11) = -2.63$, $P = 0.02$]. Furthermore, dlPFC exhibited no differential response to phobogenic (vs. neutral) images at follow-up, despite increased recruitment of this region immediately posttherapy (Fig. 1*C*, shown in red, and Table 1). This finding suggests that up-regulation of dlPFC processing, as observed in the short term (immediately after therapy), was not essential for maintaining either long-term therapy gains or long-term reduced amygdala/limbic responses to phobogenic images.

Only object-sensitive ventral visual cortex exhibited changes that emerged solely at follow-up (Fig. 2*A*, shown in gray). Activity in bilateral ventral visual cortex (fusiform/lingual gyri) was significantly greater for phobogenic than neutral images at baseline and immediately posttherapy, revealing responsivity in this region that was not immediately sensitive to therapy (Fig. 2*B* and Table 1). However, activity in this region was significantly reduced from posttherapy to follow-up [$t(11) = -5.24$, $P =$

Table 1. Summary of fMRI activity clusters

Region (BA)	L/R/B	Volume (mm^3)	*x*	*y*	*z*	Baseline, phobogenic vs. neutral *t*	Baseline, phobogenic vs. neutral *P*	Baseline vs. posttherapy *t*	Baseline vs. posttherapy *P*	Posttherapy vs. follow-up *t*	Posttherapy vs. follow-up *P*
Fig. 1, regions shown in blue											
Posterior cingulate (BA 31)	B	8,343	−4.2	36.6	40.2	1.77	0.10	−2.82	0.02	2.03	0.07
Anterior cingulate/ vmPFC (BA 24, 32)	B	7,965	2.6	−21	24.3	3.19	0.01	−3.11	0.01	NS	
Anterior insula (BA 13)	L	2,187	51.6	−8.3	−1.3	2.09	0.06	−2.70	0.02	NS	
Anterior insula (BA 13)	R	1,782	−36.9	−6.3	5.4	3.91	0.00	−2.46	0.03	NS	
Posterior insula (BA 13, 19)	R	8,478	−46.8	43.2	14.0	2.33	0.04	−2.81	0.02	NS	
Middle temporal gyrus (BA 39)	L	1,134	41.2	48.9	8.6	3.77	0.00	−2.71	0.02	NS	
Medial frontal gyrus (BA 6)	R	1,809	−5.9	10.9	61.8	2.68	0.02	−2.48	0.03	NS	
Amygdala (anatomically defined)	R	891	n/a	n/a	n/a	3.65	0.00	−4.59	0.00	NS	
Fig. 1, region shown in red											
dlPFC (BA 6, 8)	R	918	−35.6	−17.2	55.1	−2.38	0.04	8.27	0.00	−2.63	0.02
Superior parietal lobule (BA 7)	R	1,458	−24.5	66.8	55.8	NS		3.12	0.01	NS	
Fig. 2, regions shown in gray											
Fusiform/lingual gyrus (BA 18, 19)	L	8,046	−34	−81	−9	4.91	0.00	NS		−5.10	0.00
Fusiform/lingual gyrus (BA 18, 19)	R	11,367	36	−78	−11	5.14	0.00	NS		−5.36	0.00

For each activity cluster, listed are Brodmann areas (BA), hemisphere [left (L), right (R), or bilateral (B)], the volume (mm^3), and stereotactic coordinates for the centrally activated voxel (*x, y, z* mm). Statistics are reported for all *P* values ≤ 0.10, and otherwise listed as nonsignificant (NS).

0.0003], with differential activation to phobogenic vs. neutral images absent at follow-up [$t(11) = 1.57, P = 0.14$]. This pattern suggests that fear-cued enhancements in sensory cortex processing (16, 25) may represent a relatively recalcitrant phenomenon that is moderated only after gradual adjustment.

To further understand the consolidation of therapeutic gains, we sought to identify brain activity immediately after therapy that predicted lasting changes in fear moderation. We therefore identified regions in which posttherapy activity was correlated with the degree of decreased fear at follow-up. To protect against false-positives, regions were considered significant only if activity was significantly correlated across the four fear measures and only after surviving correction for multiple comparisons. This analysis identified a right-lateralized lingual gyrus subregion (Fig. 2*A*, black) within the bilateral ventral visual cortical region that showed consolidation-related activity changes (Fig. 2*A*, gray). Posttherapy activity in this subregion was significantly correlated with follow-up fear (Fig. 2*C*) [$r(10) = 0.58$, $P = 0.02$, Spider Phobia Questionnaire (SPQ); $r(10) = 0.61$, $P = 0.02$, Spider Phobia Beliefs Questionnaire (SBQ); $r(10) = 0.54$, $P = 0.04$, behavioral approach task; $r(10) = 0.58$, $P = 0.02$, fear rating]. Baseline activity in this subregion was not significantly correlated with follow-up fear (*r*-value range: −0.40 to 0.33, $P > 0.10$). In addition, baseline and posttherapy activity levels were not significantly correlated [$r(10) = 0.20, P = 0.27$]. Thus, the magnitude of visual cortex activity in this subregion that was sensitive to phobogenic stimuli immediately following therapy appeared to capture the beginning of a long-term consolidation process that

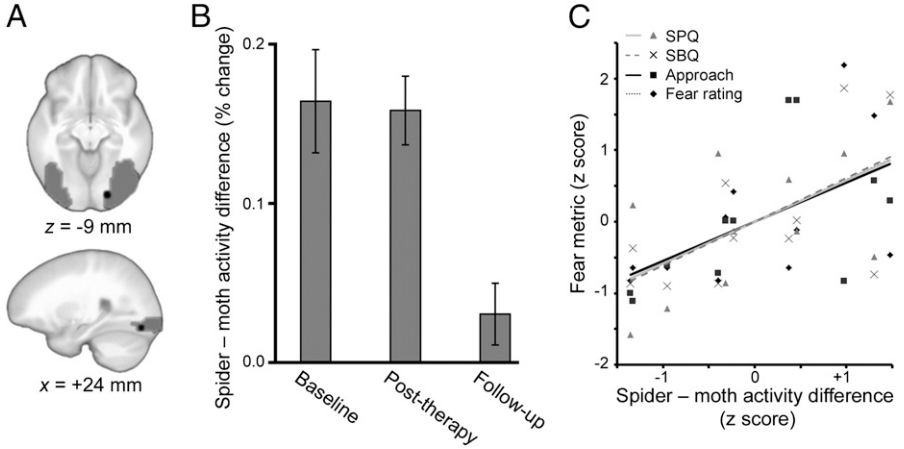

Fig. 2. Activity changes in ventral visual cortex emerged with consolidation. (*A*) The bilateral ventral visual cortical region shown in gray demonstrated significantly greater activity for phobogenic versus neutral images at baseline and immediately after therapy, but showed no differential activity (for phobogenic vs. neutral images) at follow-up due to significant activity reduction from posttherapy to follow-up (Table 1, fusiform/lingual gyrus; BA 18, 19). The right-lateralized subregion shown in black demonstrated posttherapy activity that correlated significantly with follow-up fear measures (volume = 351 mm^3; TT coordinates = +17, −82, −14; right lingual gyrus; BA 18). (*B*) Activity estimates for bilateral ventral visual cortex (shown in gray in *A*) for each scanning session. Estimates indicate mean percent signal change across all voxels in this region (for phobogenic – neutral images) during each scanning session. Error bars indicate SEM. (*C*) Neural activity in response to phobogenic (vs. neutral) images during the posttherapy scan in the right-lateralized lingual subregion (shown in black in *A*) correlated significantly with each of the behavioral fear indices at follow-up (standardized scores from each subject).

presumably occurred for bilateral ventral visual cortex, resulting in significant reductions in fear-related perceptual processing only at follow-up.

Discussion

Our results provide evidence that the beneficial effects of exposure therapy derive from neurophysiological processes typical of fear extinction. These neurophysiological processes include immediate increases in prefrontal activity in conjunction with decreases in activity of the amygdala, as well as a consolidation process that eventually allows decreased amygdala and limbic responsivity to occur independently from PFC involvement. Although neural inhibition is difficult to demonstrate in human studies, our findings show altered neural processing patterns in regions homologous to PFC-amygdala inhibitory circuitry in rodents that have undergone extinction (26). While the dlPFC subregion identified in this study does not project directly to amygdala (27), it may inhibit amygdala via projections to additional regions, particularly vmPFC–a region implicated in fear-extinction recall and considered a homolog of extinction-sensitive infralimbic structures in rodents (14, 15, 27, 28). In the present study, activity in the vmPFC was significantly decreased after therapy (Fig. S1*B*), consistent with prior studies reporting decreased vmPFC activity during classically conditioned fear extinction in humans (15). Critically, a model of dlPFC inhibition of amygdala activity, mediated via the vmPFC, has been specifically implicated in studies of cognitive reappraisal (22), a form of emotion regulation that is considered a potential mechanism for exposure therapy (29). Thus, our identification of significant posttherapy changes in the same regions brings clinical models appreciably closer into alignment with animal models of fear extinction, such that the detailed neurophysiological processes studied in animals can be linked more firmly to clinical practice.

By making use of therapy that was successfully completed in a single brief session, we were able to observe changes that occurred immediately after therapy and also compare them to results obtained 6 mo later. Neurophysiological observations shortly after therapy are vital, as activity changes in amygdala-PFC interactivity are generally identified in close proximity to fear-extinction learning (9, 10, 15). Indeed, prior neuroimaging experiments have not identified concomitant PFC-amygdala changes related to exposure therapy, perhaps because 1- to 4-wk delays were interposed between therapy completion and subsequent measurements of brain activity (30–33). In the present study, comparison between immediate and long-term effects of therapy on neural activity revealed a time-limited role of dlPFC. Because dlPFC activity is thought to reflect therapeutic techniques promoting deliberate, cognitive control of fear (22)—in particular, the dlPFC-associated technique of cognitive reappraisal mentioned above (23)—our results suggest that the utility of these cognitive techniques may be similarly time-limited. This possibility would have major implications for clinicians' approaches to understanding and refining such cognitive techniques during the course of treatment, as the degree of emphasis on such techniques in anxiety treatment has long been debated (34).

Comparison of immediate versus long-term changes also allowed us to identify a shift from "top-down" prefrontal influences to the "bottom-up" changes in visual cortex responsivity that occurred via consolidation. Presumably, this shift orchestrated the long-term reorganization of sensory processing of initially feared stimuli. Exaggerated visual cortex responses to spiders persisted even after subjects had successfully completed therapy, indicating that perceptual threat detection may be more automatic and enduring than the conscious experience of fear. Only after a longer delay did heightened perceptual activity diminish, to the point of disappearing at 6 mo. Activity in a restricted portion of the same visual cortical region immediately after therapy predicted long-term outcome, suggesting that the initial stages of this consolidation process in perceptual processing were triggered following therapy.

In characterizing the time course of neural changes that accompany therapeutic success, we identified a major brain-behavior link with respect to the elimination of anxiety symptoms and the proposed neural mechanisms previously studied in animal models. Novel aspects of recovery from phobia were highlighted by the evolution of brain responses to phobogenic stimuli, which transitioned from the baseline stage of exaggerated fear, to the initial elimination of fear a few hours later, to the final stage of a possibly permanent alleviation of symptoms. This neurophysiological evidence provides unique insights into fear-extinction mechanisms with respect to time-sensitive changes in cognitive control and threat detection, thus reinforcing the value of a neurobiologically informed perspective on anxiety disorders.

Materials and Methods

Subject Characteristics. Subjects (nine female, three male; mean age = 22.3 y, SD = 4.5 y) met diagnostic criteria for specific phobia of spiders (1), as assessed by an experienced clinician who administered the Structured Clinical Interview for DSM-IV (35). Diagnosis of specific phobia included the following symptoms: (*i*) excessive fear of spiders, (*ii*) invariable response of anxiety in the presence of spiders, (*iii*) recognition of this fear as excessive, (*iv*) consistent avoidance of spiders, (*v*) interference in daily routines due to spider fear, and (*vi*) minimum 6-mo duration of these five symptoms. For all subjects, phobia onset occurred in childhood. No subject had ever received exposure therapy or psychotropic medication. None reported fear of moths. All participants provided written, informed consent prior to their enrollment in the study. Data from one additional subject were excluded due to excessive head movement in the scanner.

Procedure. Subjects were taught the Subjective Units of Distress Scale (SUDS) (36) to communicate fear level throughout the study (score range 0–100). A range of anchors, including physiological symptoms of anxiety, was predefined on this scale to facilitate meaningful between-subjects comparisons. Subjects completed the SPQ (score range 0–31) (20) and the SBQ (score range 0–7,800) (19) to assess phobic symptom severity and catastrophic beliefs about spiders, respectively. All subjects scored in the upper 95th percentile on these questionnaires (19, 20). Subjects were then asked to approach a live Chilean Rose tarantula; the tarantula was ∼5 inches in diameter and contained in a closed terrarium at a 6.3-m distance (approach task). Ability to approach was measured as the closest distance achieved (average distance = 3.1 m from cage, SD = 1.5 m).

Subjects were then positioned for structural and functional scans. Responses to phobogenic stimuli (color photographs of spiders) versus neutral stimuli (color photographs of moths) were estimated. Stimuli were presented within a blocked design, in which 10 blocks of phobogenic stimuli alternated with 10 blocks of neutral stimuli. Each single block included five images displayed for 4 s each, followed by a 20-s rest period during which subjects used MRI-compatible buttons to enter the average fear level (SUDS) experienced while viewing the previous five images (either five spiders or five moths). To confirm that subjects perceived all stimuli, accuracy in detecting a small red square that could appear on any part of the spider or moth (for 20% of trials) was assessed. Red squares were sized and located to preclude perifoveal detection, such that fixation on the center of each spider/moth image was required to successfully perform the detection task. Subjects made a button response to each square, and responses were at least 95% accurate per scan for all subjects. Response speed did not vary as a function of stimulus type, block, or scanning session, either as a main effect (all $P > 0.33$) or as an interaction [$F(2,22) = 2.18$, $P = 0.14$]. All fMRI scans throughout the study followed the same protocol. Images were randomized across all scans without replacement, such that no image was repeated during the entire course of the experiment. Novel images decreased the possibility of habituation to phobogenic stimuli within runs, which helped to focus analyses on therapy-related changes rather than potential habituation-related changes. Post hoc RM-ANOVA analyses confirmed that habituation to images did not take place within runs [$F(1,11) = 2.46$, $P = 0.15$] and that there were no changes in habituation as a function of the run [$F(2,22) = 2.09$, $P = 0.15$].

Following the baseline fMRI scan, subjects followed one of two protocols (randomly assigned before the study day to an equal number of subjects): immediate therapy or wait control. For the immediate therapy group, remaining phases included: (*i*) exposure therapy (M = 2 h, SD = 0.5); (*ii*) posttherapy behavioral measures (SPQ, SBQ, approach task) and fMRI scan;

and (*iii*) 6-mo follow-up behavioral measures and fMRI scan. For the wait control group, remaining phases included: (*i*) waiting period (2 h), during which subjects were permitted to do anything not involving spiders or moths; (*ii*) postwait behavioral measures and fMRI scan; (*iii*) exposure therapy (M = 2 h, SD = 0.4); (*iv*) posttherapy behavioral measures and fMRI scan; and (*v*) 6-mo follow-up behavioral measures and fMRI scan.

Exposure Therapy. Exposure therapy consisted of a standard, 14-step series of progressive approach tasks (37) using the same live tarantula presented during the approach task. Each step was first demonstrated by the therapist, and the subject was then asked to repeat it when he or she felt able. Treatment was considered successful when subjects completed the final step, in which the subject touched or held the tarantula with a bare hand, with SUDS < 25. All subjects were rated as treatment successes.

fMRI Acquisition and Analysis. fMRI data were collected using a Siemens TRIO 3T MRI scanner. Functional data included whole-brain gradient-recalled echo-planar images obtained every 2 s (35 3-mm axial slices, 0-mm gap, repetition time = 2,000 ms; echo time = 25 ms; flip angle = 80°; field-of-view = 22 cm; 64 × 64 acquisition matrix; voxel size = 3.44 × 3.44 × 3 mm). High-resolution whole-brain structural images were collected to provide anatomical localization (3D MP-RAGE T1-weighted scans, voxel size = 0.859 × 0.859 × 1 mm; 160 axial slices).

fMRI analyses made use of the AFNI software package (38). For standard whole-brain analyses, preprocessing included the following: coregistration through time for motion correction, slice timing correction, removal of voxels with low signal (i.e., < 30% of mean whole-brain signal), spatial smoothing (7-mm FWHM Gaussian kernel), coregistration with the structural image, transformation to standard Talairach-Tournoux stereotactic space (Montreal Neurological Institute-305), and conversion of raw signal intensity values to percent-change values using the mean level of activity for each run. Functional and structural images were aligned across scanning sessions using a cost-function fitting approach on local correlations between signal intensities (39).

Neural activity was estimated using a standard statistical parametric mapping approach. A canonical hemodynamic response function was convolved with a 20-s boxcar function that corresponded to stimulus periods and baseline (no-stimulus) periods, with phobogenic and neutral stimulus periods modeled separately. This ideal hemodynamic timeseries was fit to the actual time series using a deconvolution analysis with a general linear model (GLM).

The GLM provided estimates of neural activity that differed for phobogenic and neutral stimuli. T_1 and T_0 components of the MRI signal and subjects' head motion in six translations and rotations were included in all GLMs as nuisance factors. Regions exhibiting group-level activation differences were identified via a two-pass random-effects analysis. Activity sensitive to phobogenic (vs. neutral) stimuli that changed between scanning sessions was tested via planned within-subjects (paired) *t* tests. RM-ANOVA results provided in Fig. S1 replicate the between-session findings of planned comparisons.

For each experimental contrast, Monte Carlo simulations were used to estimate the likelihood of detecting false positives over multiple voxel-wise comparisons (i.e., whole-brain correction). For an individual-voxel probability threshold of $P = 0.01$, the cluster-size threshold necessary to achieve an overall corrected threshold of $P = 0.01$ was identified via simulation (39). For each contrast, 30,000 simulation iterations were performed, in which two suprathreshold voxels were considered contiguous if at least one vertex was touching. The most stringent resulting cluster-size threshold of 30 voxels was applied to each contrast, to provide a conservative threshold for guarding against false positives.

An across-subjects correlation was performed between behavioral measures at follow-up and the whole-brain activity difference (for phobogenic versus neutral images) at posttherapy. One whole-brain correlation was performed for each of the four behavioral fear measures (SPQ, SBQ, approach task, fear rating), and significant regions of correlation were determined as the conjunction of the individual maps, each thresholded at a voxel-wise $r = 0.40$. Simulations performed using the same processing steps on randomly generated fMRI data matching the noise distribution of the actual data (1,000 iterations) confirmed that the resulting cluster size of 13 voxels (Fig. 2*A*) was unlikely to have been identified by chance ($P < 0.001$).

Anatomically constrained analysis was used to scrutinize amygdala activity (40, 41). For this analysis, spatial smoothing and normalization to standardized stereotactic space were not performed. The amygdala was defined in each hemisphere using the high-resolution (1-mm^3) T1 structural image for each subject in native MRI space. A 6-mm-radius sphere was centered in the middle of the amygdala, such that all amygdala nuclei were captured. The amygdala was drawn with a resolution equivalent to that of the functional images (3-mm^3 voxels). Regions of interest were aligned across scans using the transformation matrix derived from the whole-brain cost-function alignment, and anatomical alignment was confirmed visually.

ACKNOWLEDGMENTS. We thank our subjects for their laudable contributions. This study was supported by the Association for Behavioral and Cognitive Therapies Neil S. Jacobson Research Award for Outstanding and Innovative Clinical Research, the Society for a Science of Clinical Psychology Dissertation Award, Northwestern University (Graduate Research Grant, Center for Advanced Magnetic Resonance Imaging), and National Institute of Neurological Disorders and Stroke Training Grant T32 NS047987 (to K.K.H.); and by a Northwestern University Research Grant (to S.M.).

1. American Psychiatric Association (2000) *Diagnostic and Statistical Manual of Mental Disorders* (American Psychological Association, Washington, DC), 4th ed. text rev.
2. Öst LG, Alm T, Brandberg M, Breitholtz E (2001) One vs five sessions of exposure and five sessions of cognitive therapy in the treatment of claustrophobia. *Behav Res Ther* 39:167–183.
3. Öst LG, Hellström K, Kåver A (1992) One versus five sessions of exposure in the treatment of injection phobia. *Behav Ther* 23:263–281.
4. Zlomke K, Davis TE, 3rd (2008) One-session treatment of specific phobias: A detailed description and review of treatment efficacy. *Behav Ther* 39:207–223.
5. Craske MG, Mystkowski JL (2006) Exposure therapy and extinction: Clinical studies. *Fear and Learning: Basic Science to Clinical Application*, eds Craske MG, Hermans D, Vansteenwegen D (American Psychological Association, Washington, DC).
6. McNally RJ (2007) Mechanisms of exposure therapy: How neuroscience can improve psychological treatments for anxiety disorders. *Clin Psychol Rev* 27:750–759.
7. Delgado MR, Olsson A, Phelps EA (2006) Extending animal models of fear conditioning to humans. *Biol Psychol* 73:39–48.
8. LeDoux J (2003) The emotional brain, fear, and the amygdala. *Cell Mol Neurobiol* 23: 727–738.
9. Gottfried JA, Dolan RJ (2004) Human orbitofrontal cortex mediates extinction learning while accessing conditioned representations of value. *Nat Neurosci* 7:1144–1152.
10. Quirk GJ, Garcia R, González-Lima F (2006) Prefrontal mechanisms in extinction of conditioned fear. *Biol Psychiatry* 60:337–343.
11. Sotres-Bayon F, Cain CK, LeDoux JE (2006) Brain mechanisms of fear extinction: Historical perspectives on the contribution of prefrontal cortex. *Biol Psychiatry* 60: 329–336.
12. Dudai Y (2004) The neurobiology of consolidations, or, how stable is the engram? *Annu Rev Psychol* 55:51–86.
13. McGaugh JL (2000) Memory—A century of consolidation. *Science* 287:248–251.
14. Milad MR, et al. (2007) Recall of fear extinction in humans activates the ventromedial prefrontal cortex and hippocampus in concert. *Biol Psychiatry* 62:446–454.
15. Phelps EA, Delgado MR, Nearing KI, LeDoux JE (2004) Extinction learning in humans: Role of the amygdala and vmPFC. *Neuron* 43:897–905.
16. LeDoux JE (1993) Emotional memory systems in the brain. *Behav Brain Res* 58:69–79.
17. LeDoux JE (1996) *The Emotional Brain* (Weidenfeld Nicolson, London).
18. Mineka S, Mystkowski JL, Hladek D, Rodriguez BI (1999) The effects of changing contexts on return of fear following exposure therapy for spider fear. *J Consult Clin Psychol* 67:599–604.
19. Arntz A, Lavy E, van den Berg G, van Rijsoort S (1993) Negative beliefs of spider phobics: A psychometric evaluation of the Spider Phobia Beliefs Questionnaire. *Adv Behav Res Ther* 15:257–277.
20. Klorman R, Weerts TC, Hastings JE, Melamed BG, Lange PJ (1974) Psychometric description of some specific-fear questionnaires. *Behav Ther* 5:401–409.
21. Herwig U, et al. (2007) Modulation of anticipatory emotion and perception processing by cognitive control. *Neuroimage* 37:652–662.
22. Hartley CA, Phelps EA (2010) Changing fear: The neurocircuitry of emotion regulation. *Neuropsychopharmacology* 35:136–146.
23. Ochsner KN, Bunge SA, Gross JJ, Gabrieli JD (2002) Rethinking feelings: An FMRI study of the cognitive regulation of emotion. *J Cogn Neurosci* 14:1215–1229.
24. Kastner S, Ungerleider LG (2000) Mechanisms of visual attention in the human cortex. *Annu Rev Neurosci* 23:315–341.
25. Kopp B, Altmann R (2005) Neurocognitive effects of phobia-related stimuli in animal-fearful individuals. *Cogn Affect Behav Neurosci* 5:373–387.
26. Vouimba RM, Maroun M (2011) Learning-induced changes in mPFC-BLA connections after fear conditioning, extinction, and reinstatement of fear. *Neuropsychopharmacology* 36:2276–2285.
27. Delgado MR, Nearing KI, Ledoux JE, Phelps EA (2008) Neural circuitry underlying the regulation of conditioned fear and its relation to extinction. *Neuron* 59:829–838.
28. Kim MJ, et al. (2011) The structural and functional connectivity of the amygdala: From normal emotion to pathological anxiety. *Behav Brain Res* 223:403–410.
29. Tryon WW (2005) Possible mechanisms for why desensitization and exposure therapy work. *Clin Psychol Rev* 25:67–95.
30. Goossens L, Sunaert S, Peeters R, Griez EJ, Schruers KR (2007) Amygdala hyperfunction in phobic fear normalizes after exposure. *Biol Psychiatry* 62:1119–1125.
31. Paquette V, et al. (2003) "Change the mind and you change the brain": Effects of cognitive-behavioral therapy on the neural correlates of spider phobia. *Neuroimage* 18:401–409.

32. Straube T, Glauer M, Dilger S, Mentzel HJ, Miltner WH (2006) Effects of cognitive-behavioral therapy on brain activation in specific phobia. *Neuroimage* 29:125–135.
33. Schienle A, Schäfer A, Hermann A, Rohrmann S, Vaitl D (2007) Symptom provocation and reduction in patients suffering from spider phobia: An fMRI study on exposure therapy. *Eur Arch Psychiatry Clin Neurosci* 257:486–493.
34. McMillan D, Lee R (2010) A systematic review of behavioral experiments vs. exposure alone in the treatment of anxiety disorders: A case of exposure while wearing the emperor's new clothes? *Clin Psychol Rev* 30:467–478.
35. First MB, Spitzer RL, Gibbon M, Williams JBW (2002) *Structured Clinical Interview for DSM-IV-TR Axis I Disorders, Research Version, Non-patient Edition. (SCID-I/NP)* (Biometrics Research, New York State Psychiatric Institute, New York).
36. Wolpe J (1973) *The Practice of Behavior Therapy* (Pergamon Press, New York).
37. Mystkowski JL, Craske MG, Echiverri AM, Labus JS (2006) Mental reinstatement of context and return of fear in spider-fearful participants. *Behav Ther* 37:49–60.
38. Cox RW (1996) AFNI: Software for analysis and visualization of functional magnetic resonance neuroimages. *Comput Biomed Res* 29:162–173.
39. Saad ZS, et al. (2009) A new method for improving functional-to-structural MRI alignment using local Pearson correlation. *Neuroimage* 44:839–848.
40. Reber PJ, Wong EC, Buxton RB (2002) Encoding activity in the medial temporal lobe examined with anatomically constrained fMRI analysis. *Hippocampus* 12:363–376.
41. Voss JL, Hauner KK, Paller KA (2009) Establishing a relationship between activity reduction in human perirhinal cortex and priming. *Hippocampus* 19:773–778.